

Oriented Eutectic Microstructures in the System $\text{Al}_2\text{O}_3/\text{ZrO}_2$

F. SCHMID, D. VIECHNICKI

Army Materials and Mechanics Research Center, Watertown, Mass, USA

Oriented eutectic microstructures have been produced in the system $\text{Al}_2\text{O}_3/\text{ZrO}_2$ using a Bridgman-type crystal-growing furnace. Ingots consisted of elongated columnar grains or colonies. Inside the colonies a rod-type eutectic microstructure consisting of rods of ZrO_2 surrounded by an Al_2O_3 matrix was observed. The eutectic point was re-established at 63 mol % $\text{Al}_2\text{O}_3/37.0$ mol % ZrO_2 and $1870 \pm 5^\circ \text{C}$. Al_2O_3 is the first phase to nucleate when eutectic growth occurs.

1. Introduction

Oriented eutectic microstructures have been produced in systems which suggest potential applications in many areas of materials technology. Al/ Al_3Ni eutectics are of structural interest [1]. NaF/NaCl eutectics exhibit highly anisotropic optical properties [2]. Eutectic microstructures in the system $\text{BaFe}_{12}\text{O}_{19}/\text{BaFe}_2\text{O}_4$ are of interest for their magnetic properties [3]. To date the bulk of the studies on eutectic solidification have been concerned with metal systems and alkali halide systems where the temperatures involved have been relatively low, i.e. below 1000°C . High melting systems such as oxides and carbides have not been extensively investigated, yet these systems may find application where strength and hardness are required at elevated temperatures. The object of this study was to investigate eutectic solidification in some high melting oxide systems and to determine whether oriented eutectic microstructures could be produced. Viechnicki and Schmid have studied eutectic solidification in the system $\text{Al}_2\text{O}_3/\text{Y}_3\text{Al}_5\text{O}_{12}$ [4]. The system $\text{Al}_2\text{O}_3/\text{ZrO}_2$ was chosen for this study because Al_2O_3 and ZrO_2 have low vapour pressures below 2000°C [5, 6] and are not easily reduced to sub-oxides [7, 8]. Studies of phase equilibria in this system indicated that this was a simple binary system with no compound formation [9-11]. Since the position of the eutectic point was not consistent in these investigations nor was it clearly defined by v. Wartenberg *et al* [12], its position was re-investigated.

2. Experimental

2.1. Materials

The starting materials used in this investigation were alumina* and zirconia† powders. The alumina powder contained greater than 99.99% Al_2O_3 . Typical impurities listed by the producer were 0.003% Na_2O , 0.001% SiO_2 , 0.001% TiO_2 , 0.001% Fe_2O_3 , 0.001% P_2O_5 , and 0.001% Cl. The zirconia powder contained greater than 99% ZrO_2 plus HfO_2 . Maximum specific impurities listed by the producer included 0.18% SiO_2 , 0.22% CaO , 0.15% MgO , 0.10% Fe_2O_3 , 0.16% Al_2O_3 , and 0.11% TiO_2 . These powders were weighed in desired proportions, mixed in a blender for 1 h in acetone, dried and calcined for more than 72 h at 1200°C . The calcined powders were then either put directly into a Bridgman furnace for solidification studies or stored in an evacuated dessicator.

2.2. Determination of the Eutectic Point

Various compositions in the system $\text{Al}_2\text{O}_3/\text{ZrO}_2$ were mixed, pressed into small pellets, and melted in a vacuum graphite resistance furnace. Pellets were observed while they were being heated. Temperature was measured with an optical pyrometer. The temperature at which the first liquid was observed was taken to be the eutectic temperature. The eutectic composition was determined from photomicrographs of the microstructures of solidified pellets by quantitative metallography. A more complete description of the furnace and technique has been given elsewhere [13].

*Gem-242 Ultra High Purity Alumina, Engineering Materials, PO Box 363, New York 8, NY, USA.

†Zirconia A-H-C, Zirconium Corporation of America, 31501 Solon Rd, Solon 39, Ohio, USA.

2.3. Direction Solidification

90 g of calcined powder were packed into a cylindrical vapour-deposited tungsten crucible* 1.3 cm in diameter by 30 cm in length. This crucible held enough loose powder to obtain an ingot 10 cm long after an initial melting at 1900°C . Melting and directional solidification studies were done in a Bridgman crystal-growing furnace illustrated schematically in fig. 1. A helium atmosphere was used throughout this investigation. Power was supplied by a 450 kHz 20 kW rf generator to a graphite susceptor 2.5 cm in diameter and 15 cm long. Melts for solidification studies were heated to 2000°C .

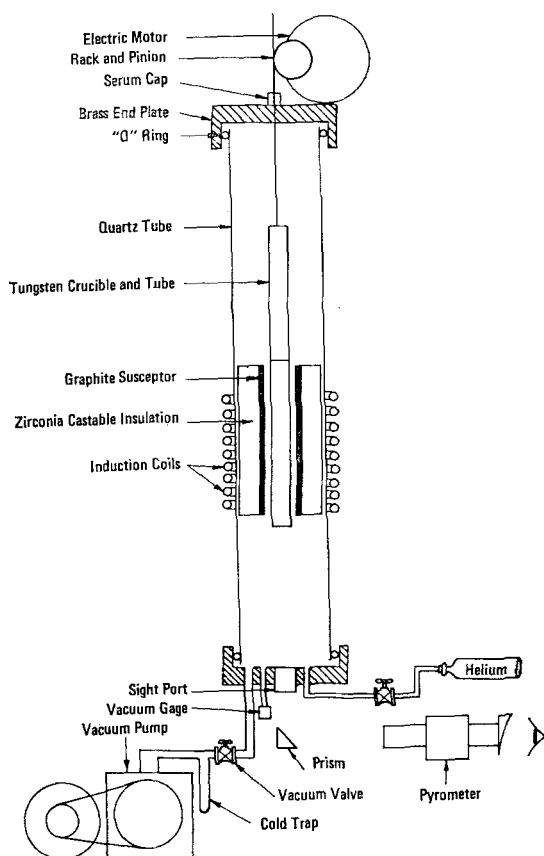


Figure 1 Schematic of Bridgman type furnace.

Cooling was accomplished by radiation from the bottom of the sample. After the initial melting and prior to further solidification studies the bottom of the tungsten crucible was cut off to eliminate a reflective interface to increase the radiation cooling. When the ingot was put into

*San Fernando Laboratories, 10258 Norris St, Pacoima, California, USA.

the furnace, its bottom was positioned to protrude 1.3 cm below the bottom of the susceptor. Thus as the power was increased, melting occurred from the top down to within 2 cm of the bottom of the ingot.

The position of the lowest liquid-solid interface relative to the bottom of the ingot could later be measured upon sectioning the ingot. Directional solidification was then accomplished by passing the crucible down through the susceptor at a given rate. Temperatures were measured from the bottom of the ingot and from the hot zone of the furnace with an optical pyrometer. Appropriate corrections were applied to obtain the actual temperatures in the furnace [13]. The temperature gradient in the solid parallel to the growth direction at the start of directional solidification was determined by taking the difference between the temperature at the bottom of the ingot and the eutectic temperature and dividing this by the distance between the bottom of the ingot and the lowest liquid-solid interface.

2.4. Optical and X-ray Studies

Polished sections were prepared using graded silicon carbide papers, diamond paste, and chromic oxide for a final relief polish. Photomicrographs were obtained from a Bausch and Lomb metallograph with a carbon arc light source. Phases present in the solidified ingots were determined by X-ray analysis using a Norelco Diffractometer and $\text{CuK}\alpha$ radiation.

3. Results and Discussion

3.1. Determination of the Eutectic Point

The following compositions were heated until a liquid phase was observed: 64.5 mol % Al_2O_3 /35.5 mol % ZrO_2 , 54.7 mol % Al_2O_3 /45.3 mol % ZrO_2 , and 49.7 mol % Al_2O_3 /50.3 mol % ZrO_2 . Liquid was first observed as these compositions were heated at $1870 \pm 5^\circ\text{C}$. This was the eutectic temperature. These solidified pellets were mounted, polished, and observed with a metallograph. The eutectic composition was determined from their microstructures. Primary Al_2O_3 and a fine rod-type eutectic microstructure was seen for the composition 64.5 mol % Al_2O_3 /35.5 mol % ZrO_2 . Primary ZrO_2 and a fine rod-type eutectic microstructure was seen for the other compositions. Fig. 2 is a cross-sectional view of this fine rod-type eutectic microstructure. ZrO_2 rods 1 μm in diameter are

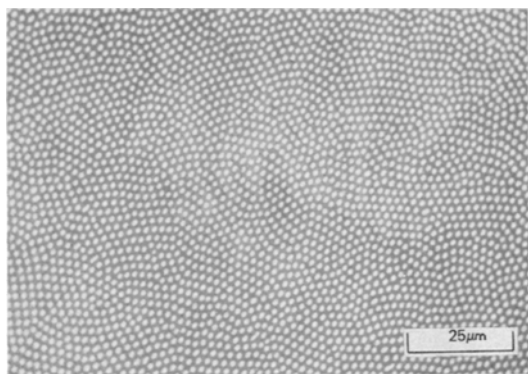


Figure 2 Transverse section of highly oriented rod-type eutectic microstructure of 63.0 mol % Al_2O_3 /37.0 mol % ZrO_2 composition.

enclosed in an Al_2O_3 matrix. Since these are the ends of rods, the area fraction of each phase was readily converted to a volume fraction and then to a mole fraction taking the density of monoclinic ZrO_2^* to be 5.56 g cm^{-3} [14]. The volume fraction, $\text{volume}_{\text{ZrO}_2}/\text{volume}_{\text{Al}_2\text{O}_3}$ was found to be 0.506 at the eutectic. The eutectic composition was thus found to be 63.0 mol % Al_2O_3 /37.0 mol % ZrO_2 . Subsequent melts of this composition had only the fine rod-type eutectic microstructure and no primary phases.

The primary Al_2O_3 in the microstructure of the 64.5 mol % Al_2O_3 /35.5 mol % ZrO_2 material served to nucleate the eutectic microstructure, whereas the primary ZrO_2 in the microstructure of the 54.7 mol % Al_2O_3 /45.3 mol % ZrO_2 material was surrounded by a ring of Al_2O_3 . Following from the findings of Sundquist and Mondolfo [15] in metal systems, it can be said that Al_2O_3 is the first phase to nucleate and causes nucleation of ZrO_2 when growth of the eutectic occurs.

H. v. Wartenberg *et al* reported a broad eutectic in the system $\text{Al}_2\text{O}_3/\text{ZrO}_2$ at 1920°C [12]. Suzuki *et al* reported the eutectic point at 50 mol % Al_2O_3 /50 mol % ZrO_2 and 1890°C . Cevalas reported the eutectic point at 62.0 mol % Al_2O_3 /38.0 mol % ZrO_2 and $1710 \pm 10^\circ \text{C}$ [10]. Alper reported the eutectic point at 64.5 mol % Al_2O_3 /35.5 mol % ZrO_2 and 1850°C [11]. The eutectic composition found in this investigation compares favourably with those reported by Cevalas and Alper. The eutectic temperature

found in this investigation compares favourably with those reported by Suzuki *et al* and by Alper. This may be considered good agreement considering the variety of methods used and the high temperatures involved.

3.2. Directional Solidification

Ingot were solidified at various growth rates between 1.29 cm h^{-1} and 15.56 cm h^{-1} . A typical ingot is one solidified at 2.59 cm h^{-1} . The temperature gradient at the start of directional solidification in the solid parallel to the growth direction was determined to be $220^\circ \text{C cm}^{-1}$. The ingot was pore-free and consisted of many columnar grains or colonies *ca.* 0.1 mm in diameter and 4 mm in length. The colonies are evident in figs. 3 and 4. Fig. 3 is a longitudinal and fig. 4 a transverse section of the ingot.

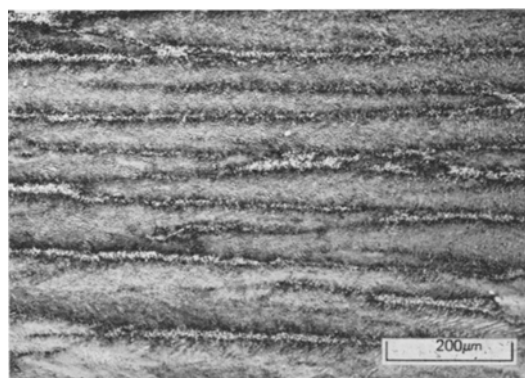


Figure 3 Longitudinal section of colony structure in an ingot of eutectic composition 63.0 mol % Al_2O_3 /37.0 mol % ZrO_2 .

Within each of the colonies was a fine oriented rod-type eutectic microstructure. Figs. 5 and 2 are the longitudinal and transverse sections of a colony. The continuous phase is Al_2O_3 . In each ingot several colonies were very highly oriented with very straight rods as seen in fig. 6. (Polishing of this section was difficult and the pitting seen in this figure could not be eliminated.) The rods are $1 \mu\text{m}$ in diameter and more than $50 \mu\text{m}$ in length.

Impurities have been shown to cause the colony structure in metal systems [16] and it is quite probable that they are the cause of the

*X-ray diffraction studies revealed that the ZrO_2 was almost totally in the monoclinic modification. A trace of a peak was noticed at $2\theta = 30.5^\circ$ which may have corresponded to a cubic (111) peak. Some small fraction of the ZrO_2 may have been in the cubic modification.

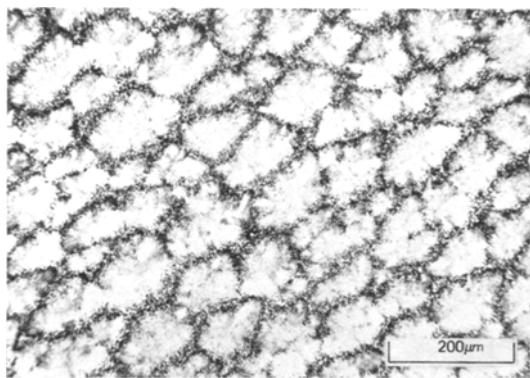


Figure 4 Transverse section of colony structure in an ingot of eutectic composition 63.0 mol % Al_2O_3 /37.0 mol % ZrO_2 .

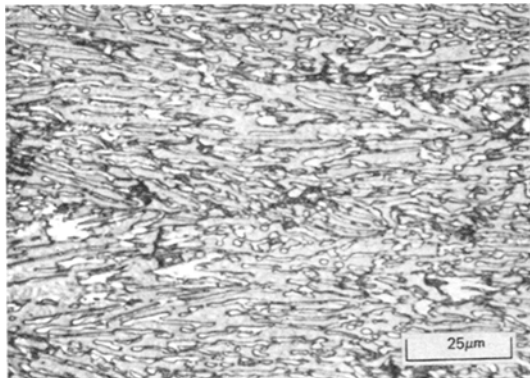


Figure 5 Longitudinal section of eutectic microstructure of 63.0 mole % Al_2O_3 /37.0 mol % ZrO_2 composition.

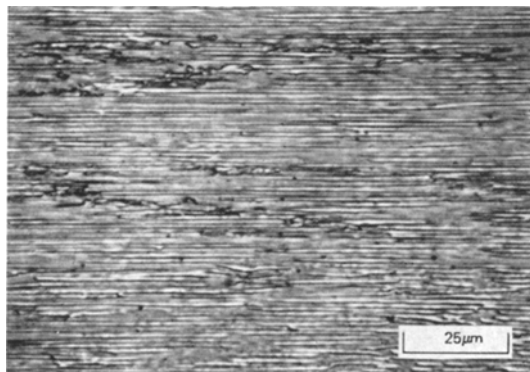


Figure 6 Longitudinal section of highly oriented rod-type eutectic microstructure of 63.0 mol % Al_2O_3 /37.0 mol % ZrO_2 composition.

colony structure in the $\text{Al}_2\text{O}_3/\text{ZrO}_2$ system, considering the relatively impure starting materials, 99.99% pure Al_2O_3 and 99% pure ZrO_2 . The high temperatures required for melting probably caused some contamination from the tungsten crucibles [4]. Radial temperature gradients and local temperature gradients caused by the rejection of impurities ahead of the growing liquid-solid interface further complicated controlled growth of these eutectics. Highly oriented eutectic microstructures are obtainable in the system $\text{Al}_2\text{O}_3/\text{ZrO}_2$, but it appears that cleaner starting materials and higher experimentally imposed temperature gradients may be necessary to grow these eutectics in a controlled manner.

References

1. F. O. LEMKEY, R. W. HERTZBERG, and J. A. FORD, *Trans. Met. Soc. AIME* **233** (1965) 334.
2. J. A. BATT, F. C. DOUGLAS, and F. S. GALASSO, *Amer. Ceram. Soc. Bull.* **48** (1969) 622.
3. F. S. GALASSO, W. L. DARBY, F. C. DOUGLAS, and J. A. BATT, *J. Amer. Ceram. Soc.* **50** (1967) 333.
4. D. VIECHNICKI and F. SCHMID, *J. Mater. Sci.* **4** (1969) 84.
5. C. B. ALCOCK and M. PELEG, *Trans. Brit. Ceram. Soc.* **66** (1967) 217.
6. R. J. ACKERMANN and R. J. THORN, in "Progress in Ceramic Science, I" (Pergamon Press, New York, 1961) p. 66.
7. H. YANAGIDA and F. A. KRÜGER, *J. Amer. Ceram. Soc.* **51** (1968) 700.
8. R. F. DOMAGALA and D. J. MCPHERSON, *Trans. Met. Soc. AIME* **200** (1954) 238.
9. H. SUZUKI, S. KIMURA, H. YAMADA, and T. YAMAUCHI, *J. Cer. Assoc. Japan* **69** (1961) 52.
10. G. CEVALES, *Ber. Dtsch. Keram. Ges.* **45** (1968) 216.
11. A. ALPER, private communication, 7 August 1969.
12. H. V. WARTENBERG, H. LINDE, and R. JUNG, *Z. anorg. allg. Chem.* **176** (1928) 349.
13. D. VIECHNICKI and F. SCHMID, *Mat. Res. Bull.* **4** (1969) 129.
14. A. SILVERMAN, Data on Chemicals for Ceramic Use, National Research Council. (National Academy of Science, Washington, DC, June, 1949).
15. B. E. SUNDQUIST and L. F. MONDOLFO, *Trans. Met. Soc. AIME* **221** (1961) 157.
16. B. CHALMERS, "Principles of Solidification" (Wiley, New York, 1964) p. 207.
17. *Ibid.*, p. 150.

Received 6 October 1969 and accepted 2 March 1970.